



# Performance Review of Mt. Lorne Photovoltaic (PV) Array From June 1 to December 31, 2019

**Prepared by:**

Christopher Baldus-Jeursen

CanmetENERGY in Varennes

[christopher.baldus-jeursen@canada.ca](mailto:christopher.baldus-jeursen@canada.ca)

**Presented to:**

Renewable Energy Integration Group

Mt. Lorne Project Partners

Date: September 13, 2020

### **Disclaimer**

Natural Resources Canada (NRCan) is not responsible for the accuracy or completeness of the information contained in the reproduced material. NRCan shall at all times be indemnified and held harmless against any and all claims whatsoever arising out of negligence or other fault in the use of the information contained in this publication or product.

### **Copyright**

Information contained in this publication or product may be reproduced, in part or in whole, and by any means, for personal or public non-commercial purposes, without charge or further permission, unless otherwise specified.

You are asked to:

- exercise due diligence in ensuring the accuracy of the materials reproduced;
- indicate the complete title of the materials reproduced, and the name of the author organization; and
- indicate that the reproduction is a copy of an official work that is published by Natural Resources Canada (NRCan) and that the reproduction has not been produced in affiliation with, or with the endorsement of, NRCan.

Commercial reproduction and distribution is prohibited except with written permission from NRCan. For more information, contact NRCan at [copyright.droitdauteur@nrcan-rncan.gc.ca](mailto:copyright.droitdauteur@nrcan-rncan.gc.ca).

*© Her Majesty the Queen in Right of Canada, as represented by the Minister of Natural Resources Canada, 2020.*

## Summary

The Mt. Lorne PV array near Whitehorse, Yukon, was installed in February 2017 and was complemented with a monitoring system in May 2019. The study of array performance by CanmetENERGY in Varennes provides data that guide the development and deployment of PV in northern Canadian communities and reduces their dependence on fossil fuels. The monitoring campaign for the Mt. Lorne array, from June 1 to December 31, 2019, reported a total energy production of 23.6 MWh. Using typical hydro electric rates for the region as a reference, this corresponded to \$2826 saved. Closer inspection revealed five likely failed inverters that are reducing array power output by approximately 12%.

# Table of Contents

<b>1</b>	<b>System synopsis .....</b>	<b>1</b>
<b>2</b>	<b>Solar insolation at high latitudes.....</b>	<b>2</b>
<b>3</b>	<b>Annual, monthly, and daily performance indicators .....</b>	<b>6</b>
<b>4</b>	<b>Influence of array shading and snow accumulation on performance.....</b>	<b>9</b>
<b>5</b>	<b>Conclusions .....</b>	<b>10</b>
<b>6</b>	<b>Appendix.....</b>	<b>12</b>
	6.1 Array foundations and installation .....	12
	6.2 Array monthly output .....	13
<b>7</b>	<b>References .....</b>	<b>16</b>

## List of Tables

Table 1 : Summary of site and array with temperature and irradiance data reported from the CanmetENERGY monitoring kit from June 1 to December 31, 2019. ....	2
Table ii : Performance metrics and meteorological figures (GHI REF is the insolation from the nearest CWEEDS station). Totals were obtained using data that was rounded to the nearest integer.....	11

## List of Figures

Figure 1 : Mt. Lorne PV array [photo credit: Total North Communications].....	1
Figure 2 : Sunrise, sunset and hours of sunshine with discontinuities on March 10 and November 3 indicating the start and end of daylight savings time, respectively. ....	3
Figure 3 : Cartesian coordinate sun path chart for Mt. Lorne with hour lines shown in local standard time. ....	3
Figure 4 : Comparison between measured Apogee SP 510 insolation and monthly CWEEDS averages .....	4
Figure 5 : Comparison between global horizontal irradiance and clear sky model. ....	5
Figure 6 : Monthly array performance for 2019. Temperature corrected performance ratio (%) is shown above each bar.....	7
Figure 7 : Average normalized branch power output during two summer months .....	8
Figure 8 : SAM 3-D shade calculator view of the Mt Lorne array on February 4, 2019 at 16h00 LST with a shade fraction of 13.4%.....	9
Figure 9 : Average hour-by-month direct-beam irradiance losses for the entire array. Complete shade is shown as 100% and no shading is 0%. ....	10
Figure 10 : Array foundation installation and levelling [photo credit: Total North Communications] .....	12

# 1 System synopsis

The PV array is located at the Mount Lorne Waste Transfer Station, near the city of Whitehorse, Yukon. A summary of geographic features and system components is given in Table 1. Designed and installed by Total North Communications, the array consists of 162 modules with a total nameplate power of 50.22 kW. The modules' construction consists of 6 x 20 crystalline silicon half-cut cells in monofacial format, a composite film backsheet, and pre-stressed glass cover with anti-reflection technology. The mounting configuration consists of four racks of 36 modules each, and a fifth rack of 18 modules. The racking structure is installed in sandy soil using 46 inch screw-in ground anchors [1]. A photo of the foundation can be found in the Appendix.



**Figure 1** : Mt. Lorne PV array [photo credit: Total North Communications]

The array uses 41 microinverters which provide a higher level of performance and monitoring than traditional string inverters when the array is partially shaded. Each microinverter has inputs for four modules with a separate connection to the AC mains bus. There are 40 microinverters each connected to 4 modules, and 1 microinverter connected to 2 modules. Microinverter outputs are grouped into 11 circuit branches. There are 9 branches with 4 inverters, and 2 branches with 3 inverters. Circuit branches run through trenches from the array to the AC disconnect board and terminate at the AC breaker panel located in a nearby equipment building. Built by Total North, the building provides a sheltered area for electronic equipment, is equipped with an electric vehicle charging station, and hosts the CanmetENERGY monitoring kit with pole-mounted pyranometers and

ambient temperature sensor. The monitoring kit averages data at 15 minute intervals providing the following parameters: global horizontal and plane of array irradiance, ambient temperature, and power metrics for each branch from which the total system output power is derived. These data may be supplemented with data at the micro-inverter level available online from AP systems. The difference between the monitoring kit and AP systems power output measured at the inverter exceeds the 2-3% difference expected due to resistive cabling losses between the microinverters and the monitoring kit. Thus, only data from the monitoring kit are used in this report until AP systems provides more information on the quality of their data.

**Table 1** : Summary of site and array with temperature and irradiance data reported from the CanmetENERGY monitoring kit from June 1 to December 31, 2019.

Geographic Features	PV Array Configuration
Location: Mount Lorne (Whitehorse), Yukon	Array installation : February 2017
Altitude: 768 m	Module: Q Peak Duo BLK-5G, 310 (Hanwa Q-cell)
Latitude: 60.5°N	Azimuth: 180° (aligned to geographic north)
Longitude: 134.9°W	Tilt: 45°
Maximum dry bulb temperature 2019: 30.9°C	Inverter topology: 41 micro-inverters
Minimum dry bulb temperature 2019: - 30.8°C	Inverter type: YC1000-3, AP systems
Monthly POA max: 154 kWh/m <sup>2</sup> /month	Radiometer: Apogee SP 510 (POA, GHI)
Monthly POA min: 12 kWh/m <sup>2</sup> /month	Monitoring kit installation: May 2019

## 2 Solar insolation at high latitudes

Operation of PV arrays in cold climates often entails lower light levels and higher angles of incidence during the winter season, elevated UV content at high altitude, colder cell temperatures, and snow and ice accumulation. Compared to warmer climatic zones, the solar resource at high latitudes generally has reduced sunlight hours during winter operation. The length of the day varies with latitude and season. For Mt. Lorne, Figure 2 shows the calculated sunrise and sunset time and the number of hours of daylight. The longest day occurs on June 21 at the summer solstice and is approximately 19 hours long. The shortest day occurs on December 21 during the winter solstice and is only 5 hours and 43 minutes. The trajectory of the sun across the sky is also important to study the effects of array self-

shading as a function of solar elevation and solar azimuth angle, and to consider reflectance losses at high angles of incidence. Sun path charts for Mt. Lorne were generated by a program available from the University of Oregon Solar Radiation Monitoring Laboratory [2].

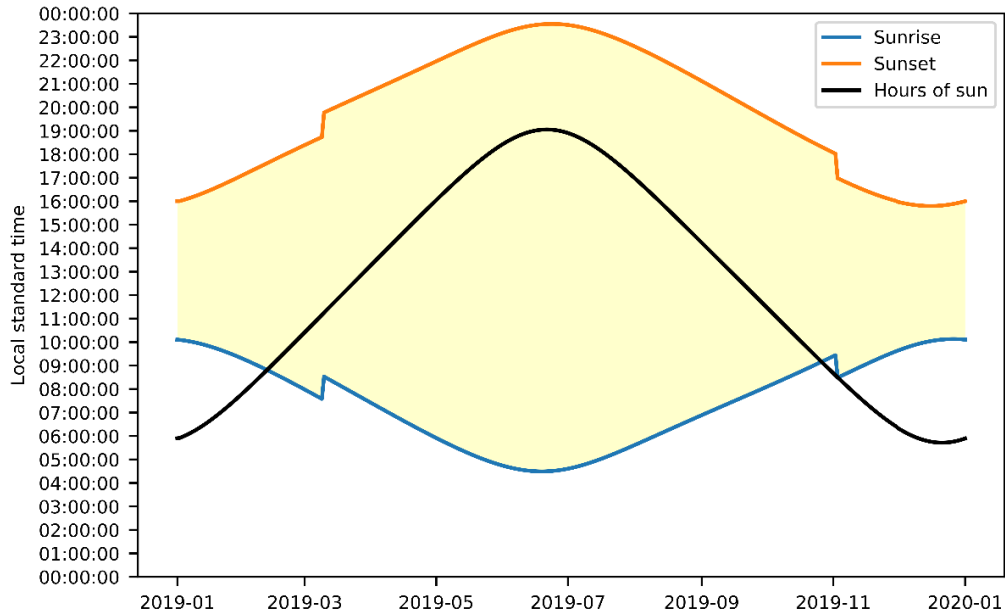


**Figure 2 :** Sunrise, sunset and hours of sunshine with discontinuities on March 10 and November 3 indicating the start and end of daylight savings time, respectively.

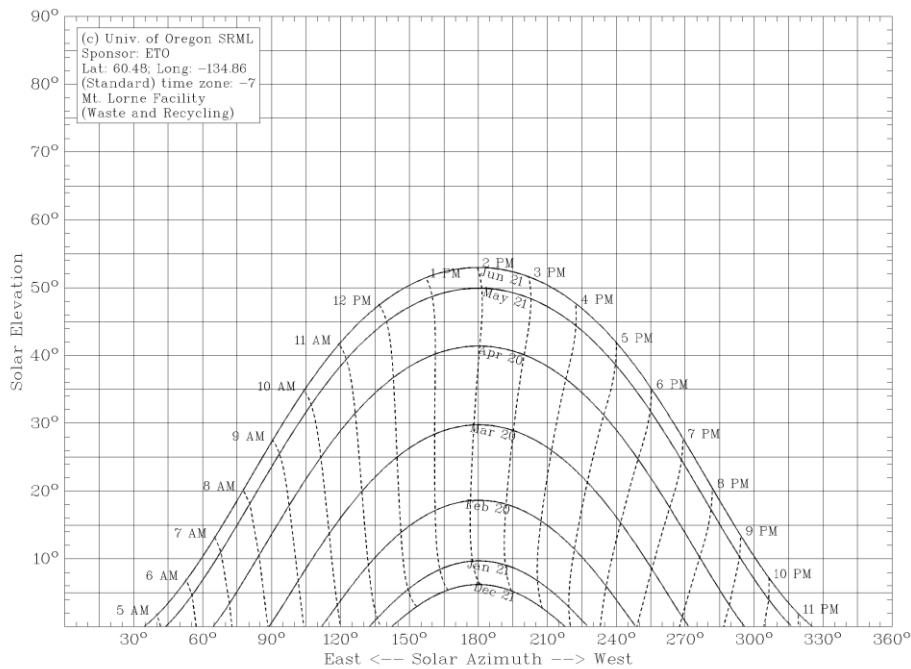
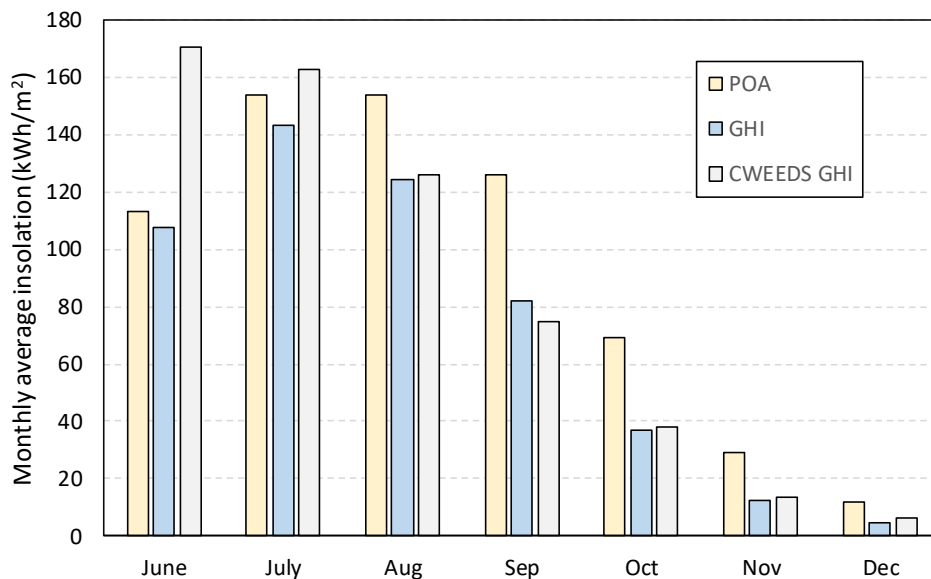


**Figure 3 :** Cartesian coordinate sun path chart for Mt. Lorne with hour lines shown in local standard time.



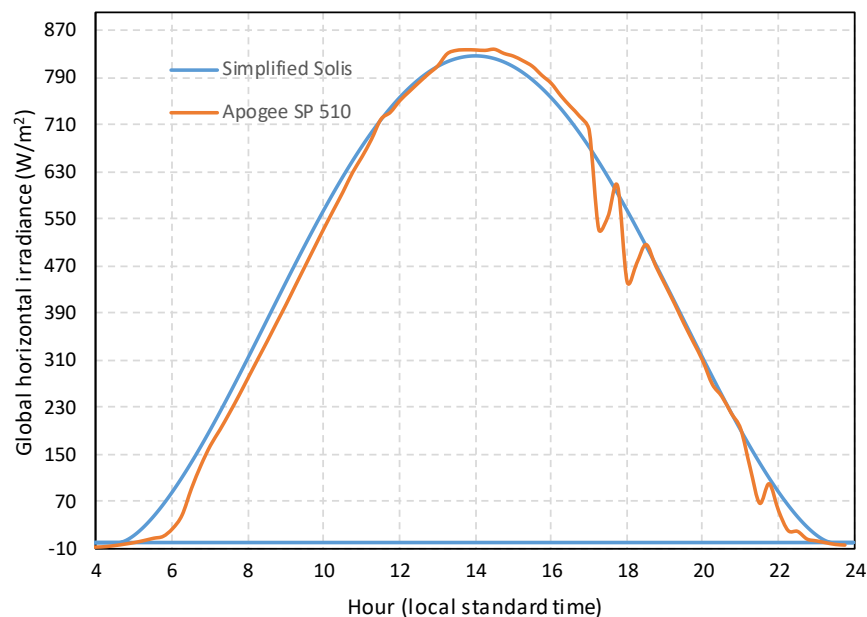
As shown in Figure 3, the sun’s path during the winter months is relatively low on the horizon. The solar elevation angle is approximately 6° at the winter solstice, and reaches a maximum of around 53° at the summer solstice. The low elevation angle leads to self-shading by some rows of the array. Shading considerations are examined in a separate section of this report. Furthermore, during summer in the northern hemisphere, the sun rises in the north east and sets in the north west. At summer solstice, for example, the sun rises at a solar azimuth angle of approximately 35° and sets at an angle of 325°. That is, the sun rises and sets behind the array. By contrast, in winter, the sun rises in the south east and sets in the south west in front of the array.

Figure 4 shows the horizontal and plane of array monthly insolation as measured by the Apogee SP 510. Also shown in Figure 4, for comparison purposes, is the average horizontal insolation measured at CWEEDS station # 2101303 in Whitehorse using data from 2005 to 2017. Apogee insolation for June was slightly underreported due to an eight-day outage from June 20 to June 27. Outages may have been caused due to datalogger malfunction or local grid downtime. Maximum insolation occurred during July and August with a minimum in December. The total plane of array insolation from June to December was 657 kWh/m<sup>2</sup>.



**Figure 4 :** Comparison between measured Apogee SP 510 insolation and monthly CWEEDS averages

In order to quality check the Apogee data on the horizontal, a comparison was made using the Sandia Simplified Solis clear sky model. The Simplified Solis model requires as inputs both the aerosol optical depth at 700 nm, and the precipitable water vapour. An appropriately sunny day on June 14 was chosen for the analysis. Aerosol optical depth data for that day were collected from the Kluane Lake measurement site using the Aeronet Aerosol Robotic Network (an international federation of ground-based remote sensing networks) [3]. Precipitable water vapour data were collected from atmospheric soundings from the city of Whitehorse (WMO station ID 71964) [4]. Apogee data versus the clear sky prediction are shown in Figure 5, and agree within 2% at peak irradiance. These results indicate the Apogee SP510 is accurate on the horizontal.



**Figure 5 :** Comparison between global horizontal irradiance and clear sky model.

As shown by the nighttime data from the Canmet monitoring system, when tilted at 45° the Apogee has slightly reduced thermal offset since it sees more of the ground and less sky. Single digit negative nighttime readings for thermopile pyranometers are normal due to infrared radiative transfer between the warm pyranometer black disk receiver and the cold sky. Uncertainties due to tilt are added in quadrature to the uncertainties present on the horizontal. The uncertainty of a tilted pyranometer will always be slightly greater than that of a corresponding GHI measurement from the same instrument [5].

### 3 Annual, monthly, and daily performance indicators

Array performance was analyzed by dividing energy output losses into different categories. The assessment of the performance of any array begins with determining the amount of incident energy over a given time period. In this case, data were collected at 15-minute intervals, but cumulative totals were also calculated over hourly, daily, and monthly periods. The amount of incident insolation relative to standard test conditions is defined as the reference yield,  $Y_R$ , given by equation 1,

$$Y_R = H_G / G_o \quad (1)$$

where  $H_G$  is the incident insolation over the reference time period, and  $G_o$  is the irradiance under standard test conditions ( $1000 \text{ W/m}^2$ ). The array yield,  $Y_A$ , is defined as the DC energy produced over the reference period,  $E_A$ , divided by the nameplate power,  $P_o$ , as given by equation 2.

$$Y_A = E_A / P_o \quad (2)$$

The final yield,  $Y_F$ , is defined as the AC energy produced over the reference period,  $E_F$ , divided by the nameplate power,  $P_o$ , as given by equation 3. By normalizing to nameplate power, comparison between arrays of different sizes become possible.

$$Y_F = E_F / P_o \quad (3)$$

The difference between the reference yield and the array yield is defined as capture loss. Capture loss is divided into two categories: thermal loss due to the array operating above  $25^\circ\text{C}$ , and miscellaneous losses. Miscellaneous losses are not temperature dependent and refer to, for example:

- Inhomogeneous irradiance from soiling (dust buildup, snow), partial shading
- Wiring losses, module mismatch, maximum power point tracking errors
- Low irradiance or high angle of incidence, pyranometer inaccuracies or spectral effects

By contrast, system losses are defined as the difference between the final yield and the array yield. Thus, system losses quantify inverter conversion efficiency (or equivalently battery conversion losses for a stand-alone system). For this report, the average inverter efficiency of 94.5% from the YC1000-3 data sheet was used to calculate system losses. By dividing the system yield by the reference yield, the system performance ratio, PR, can be calculated. The PR is an important metric of array performance

because it compares the actual yield from the array to the ideal yield measured by the radiometer, thus highlighting overall losses and system quality. Typical PR values for normal operation range from 75% up to 90%. Based on the energy produced, estimates were made for the amount of money saved. The Yukon generates approximately 94% of its electricity from hydro electric sources. To convert from array energy production to money saved, an estimated hydroelectric rate of 12 c/kWh was used [6]. Performance ratio, energy produced, final yield, and system and capture losses are shown for a partial year of data collection in Figure 6. Similar graphs for a monthly time scale are given in the Appendix.

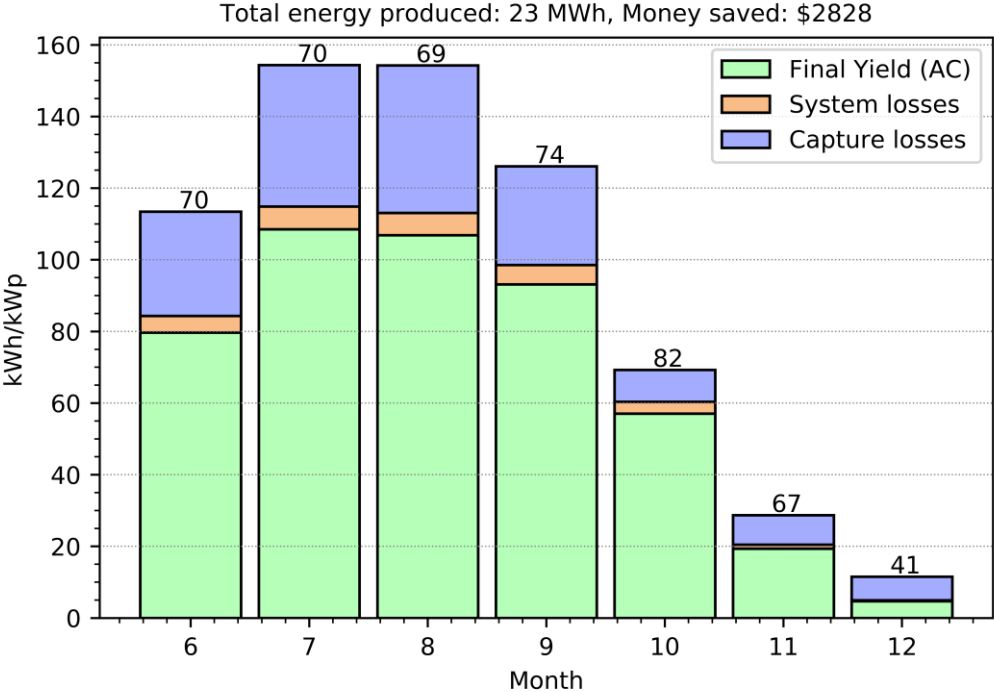
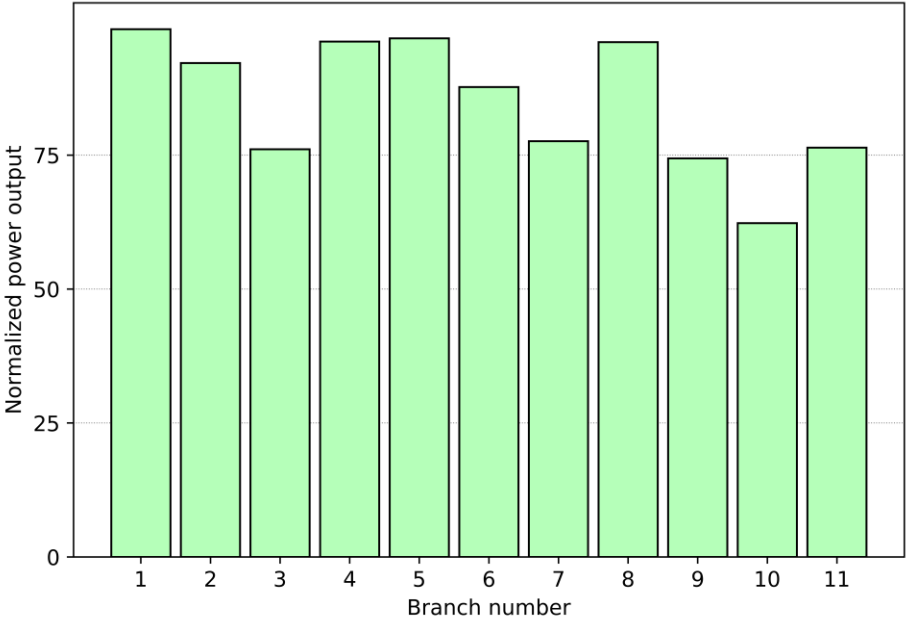


Figure 6 : Monthly array metrics for 2019. Performance ratio (%) is shown above each bar.

Seasonal variations in temperature have an effect on array output voltage. Relative to 25°C standard test conditions, warm summer temperatures may result in slightly lower PR whereas colder fall and winter temperatures may increase PR. Peak months of production were in June, July, August, and September with steadily declining production in October, November, and December. During the summer months, performance ratio was around 70% which was somewhat low compared to a normally operating array. In order to determine the cause of the discrepancy, power output was analyzed for all eleven branches for every day in July and August using output measured near solar noon. The predicted output power for each branch was calculated in two steps: 1) by calculating the

maximum power produced as a function of temperature and irradiance for a generic crystalline silicon module using a formula validated in previous field tests [7], and 2) applying typical losses for wiring, connections, inverter efficiency, and module ageing. The average measured power for each branch normalized by the expected power is shown in Figure 7. Based on these results, branches 3, 7, 9, 10, and 11 were underperforming. Given that each of these branches have four microinverters, it is notable that four branches had normalized output very close to 75% which implies the failure of one inverter per underperforming branch. Thus, it is strongly suspected that five inverters have failed corresponding to a lost output from 20 modules or around 12% of the array. These failed inverters explain the reduced performance ratio evident during the summer months. It should also be noted that the AP systems website for the array shows a variety of non-communicating inverters some of which reestablish communication after several days. However, some non-communicating inverters on the website still appear to operate normally and supply power to the grid.



**Figure 7 :** Average normalized branch power output during two summer months

While PR values are slightly reduced during the summer, there is a much greater decline in PR during the winter months which can be explained by a combination of snowfall and array shading at high angles of incidence.

## 4 Influence of array shading and snow accumulation on performance

Although there are no direct measurements of snowfall at the Mt. Lorne site, data on snow depth measured by ruler are available 30 km away at the Whitehorse precipitation station (CWEEDS station ID 2101303) from 2005 to 2012. This station routinely shows snowfall beginning in early October and ending in mid-April, with maximum snow depths of up to 45 cm. Snow losses can be simulated using the System Advisor Model (SAM) program available from the National Renewable Energy Laboratory (NREL). SAM has two excellent features for calculating shading losses: a row-on-row shading algorithm used primarily for large commercial systems where the shading effects are linear and uniform, and a detailed 3-D shading tool for smaller systems such as residential arrays where non-uniform shading effects are modeled. The 3-D shading tool was used to analyze the Mt. Lorne system starting with a satellite image of the site with corresponding length scale onto which building shading objects and the PV array active surfaces were placed. Array active surfaces show self-shaded areas

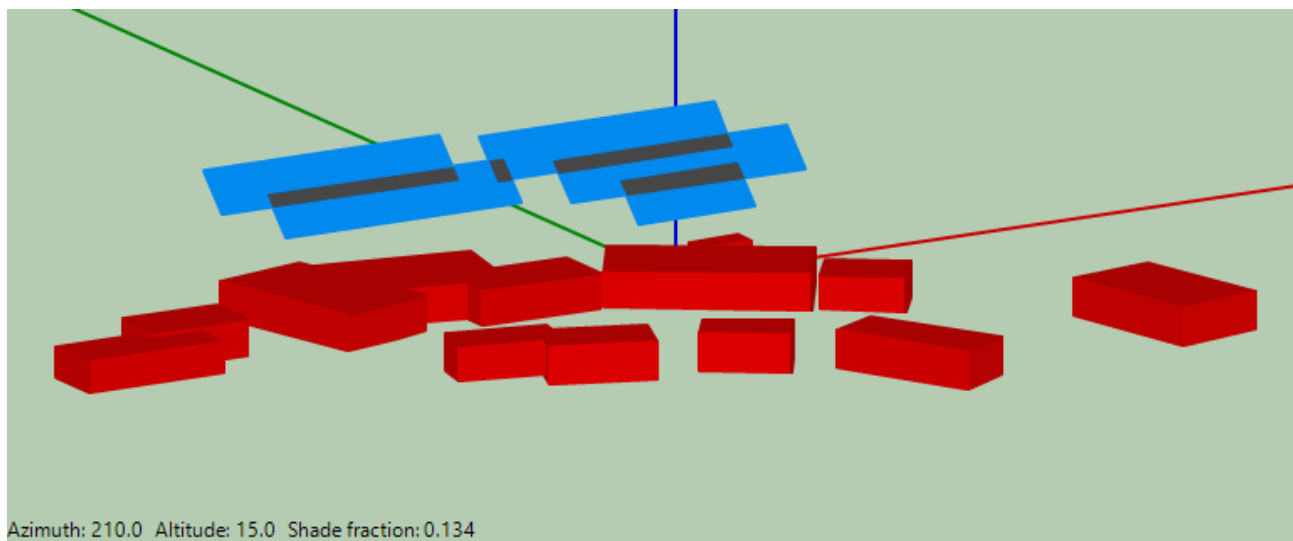


**Figure 8** : SAM 3-D shade calculator view of the Mt Lorne array on February 4, 2019 at 16h00 LST with a shade fraction of 13.4%.

in dark blue. The effects of trees were ignored. However, spring and summer foliage growth could be taken into account if additional site photos are collected. SAM uses a solar position algorithm to generate hour-by-month direct-beam and diffuse irradiance loss percentages. Electrical simulation of the array is not possible at this stage since SAM weather files require a complete year of data including

wind speed for cell temperature calculations. However, the 3-D shading tool provides insight into irradiance losses. For example, Figure 8 shows the self-shading of the array rows for direct-beam irradiance at a given solar elevation and azimuth. The analysis of shading losses shown in hour-by-month averages for the entire array is given in Figure 9.

	12 AM	1 AM	2 AM	3 AM	4 AM	5 AM	6 AM	7 AM	8 AM	9 AM	10 AM	11 AM	12 PM	1 PM	2 PM	3 PM	4 PM	5 PM	6 PM	7 PM	8 PM	9 PM	10 PM	11 PM	
Jan	100	100	100	100	100	100	100	100	100	100	100	42	34	34	32	32	42	100	100	100	100	100	100	100	100
Feb	100	100	100	100	100	100	100	100	100	100	27	20	17	17	16	16	18	22	36	100	100	100	100	100	100
Mar	100	100	100	100	100	100	100	100	24	2	1	0	1	0	1	1	1	2	4	6	100	100	100	100	100
Apr	100	100	100	100	100	100	100	100	4	0	0	0	0	0	0	0	0	0	0	0	0	100	100	100	100
May	100	100	100	100	100	100	100	100	1	0	0	0	0	0	0	0	0	0	0	0	0	100	100	100	100
Jun	100	100	100	100	100	100	100	100	1	0	0	0	0	0	0	0	0	0	0	0	0	100	100	100	100
Jul	100	100	100	100	100	100	100	100	1	0	0	0	0	0	0	0	0	0	0	0	0	100	100	100	100
Aug	100	100	100	100	100	100	100	100	3	0	0	0	0	0	0	0	0	0	0	0	0	100	100	100	100
Sep	100	100	100	100	100	100	100	100	7	0	0	0	0	0	0	0	0	0	0	0	0	100	100	100	100
Oct	100	100	100	100	100	100	100	100	19	12	10	10	9	9	10	12	16	21	100	100	100	100	100	100	100
Nov	100	100	100	100	100	100	100	100	100	39	31	29	28	26	28	36	100	100	100	100	100	100	100	100	100
Dec	100	100	100	100	100	100	100	100	100	100	50	39	39	36	42	68	100	100	100	100	100	100	100	100	100

**Figure 9** : Average hour-by-month direct-beam irradiance losses for the entire array. Complete shade is shown as 100% and no shading is 0%.

During the summer months, shading losses are less than 3%. Shading losses increase substantially during the fall and winter months. During January, February, October, November, and December, the array is often partially shaded even during solar noon. Also, periods which are shown as 100% direct-beam shaded do not necessarily mean that the array is not producing power. For example, during early morning periods during the summer, the sun will rise and set behind the array but there will still be diffuse irradiance from clouds and surrounding terrain. During the winter months, reflection/albedo from snow will enhance array output.

## 5 Conclusions

Array performance was analyzed to determine energy output, performance ratio, and money saved. A uniform reduction in the performance ratio, while masked during winter operation by array self-shading and snow coverage, was evident during the summer months. This performance reduction of approximately 12% is explained by five inverter failures corresponding to lost output from 20 modules. The array must be monitored regularly to track additional failures and to ensure timely replacement of faulty inverters if needed. Table ii summarizes all the performance metrics for each

month and for the total period under investigation. In 2020, the first full year of data for the Mt. Lorne site will be obtained and annual reports will follow.

**Table ii** : Performance metrics and meteorological figures (GHI REF is the insolation from the nearest CWEEDS station). Totals were obtained using data that was rounded to the nearest integer.

Month	Energy (kWh)	Yield (kWh/kWp)	POA (kWh/m <sup>2</sup> )	GHI (kWh/m <sup>2</sup> )	GHI REF (kWh/m <sup>2</sup> )	PR	Money Saved (\$)
June	4001	79	113	108	171	70	480
July	5450	108	154	143	163	70	654
Aug	5367	106	154	124	126	69	644
Sep	4677	93	126	82	75	74	561
Oct	2865	57	69	37	38	82	343
Nov	972	19	29	12	134	67	116
Dec	234	4	12	4	6	41	28
Total	23566	466	657	510	713	71	2826



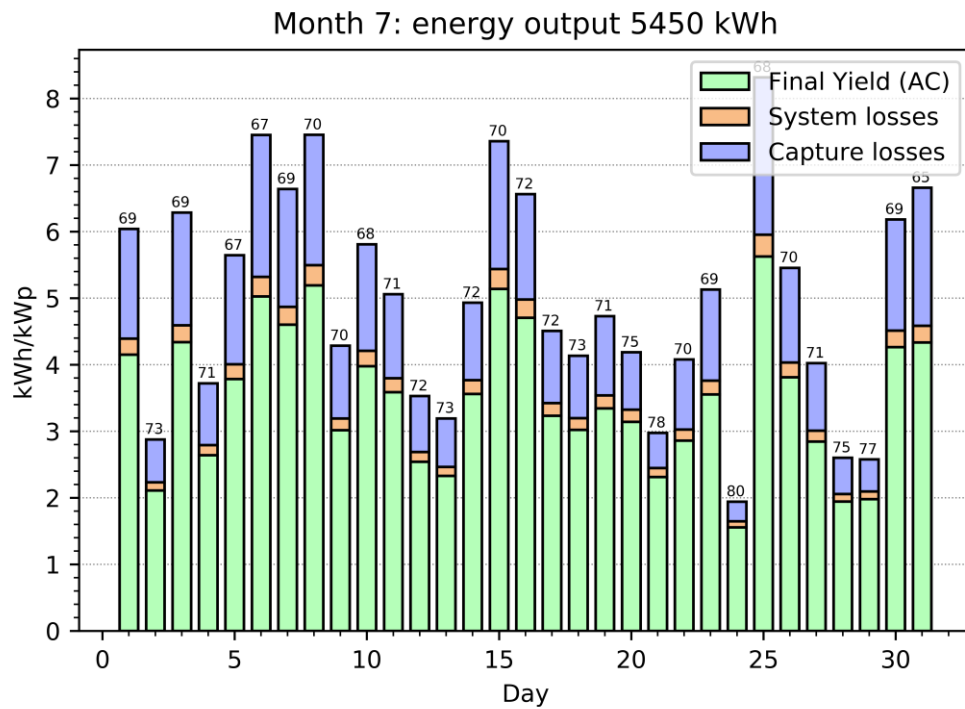
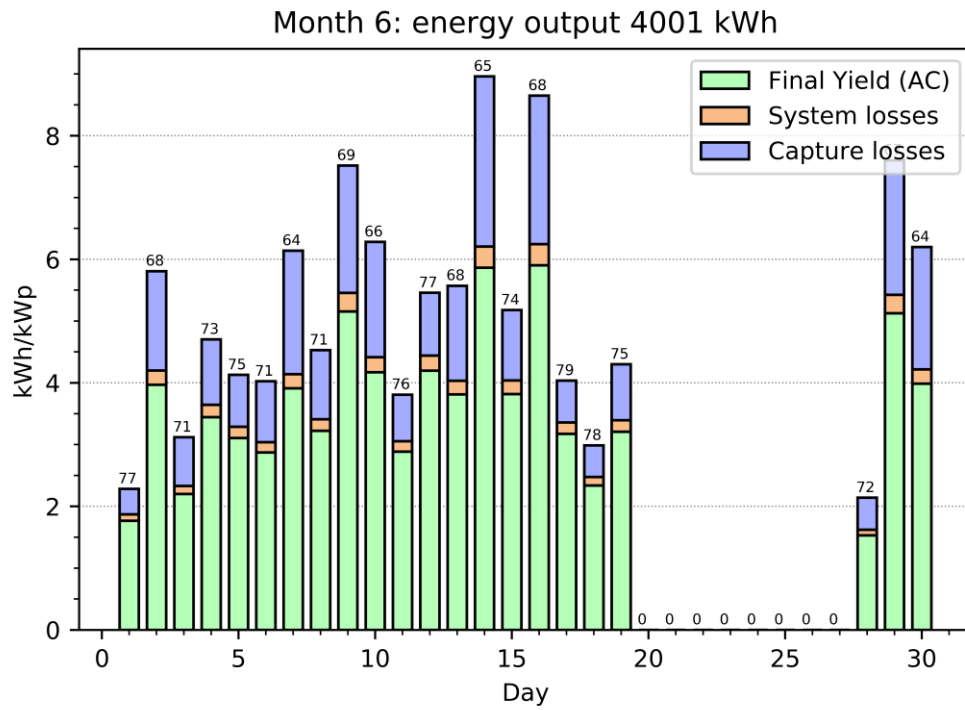
## 6 Appendix

### 6.1 Array foundations and installation

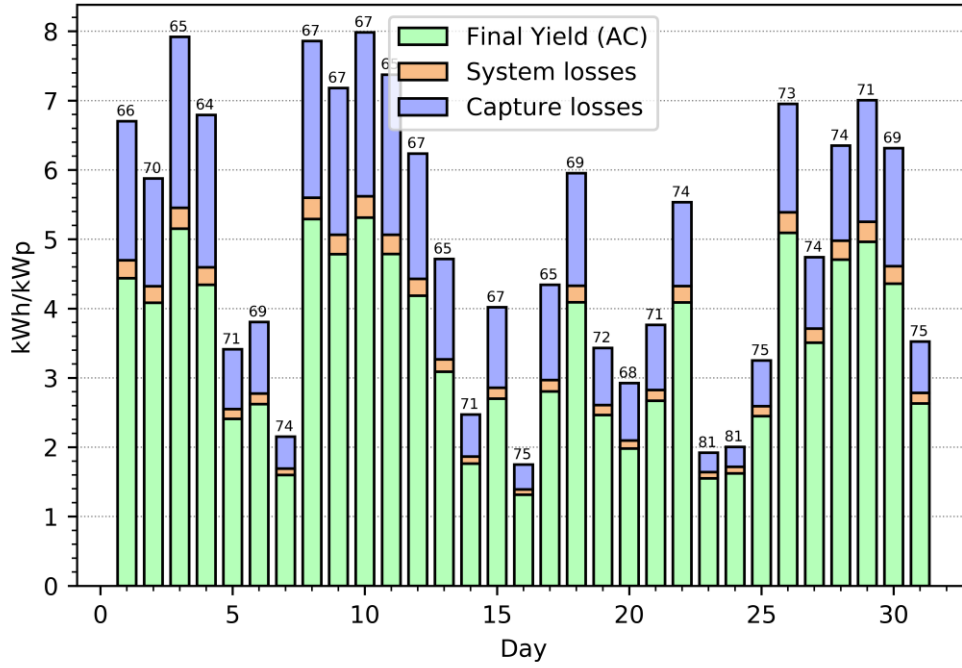


**Figure 10** : Array foundation installation and levelling [photo credit: Total North Communications]

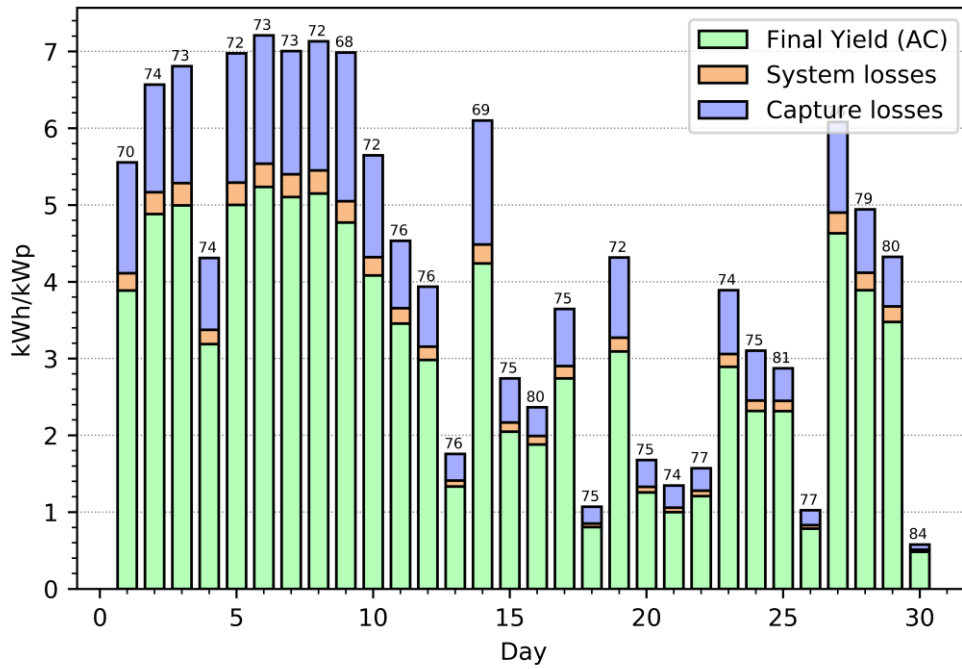
## 6.2 Array monthly output



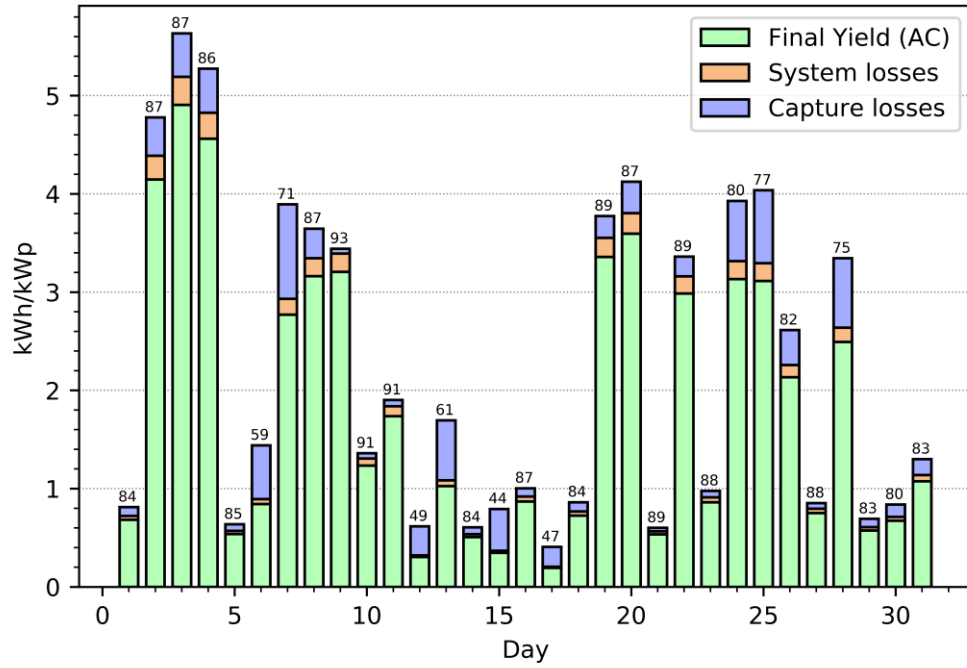
Month 8: energy output 5367 kWh



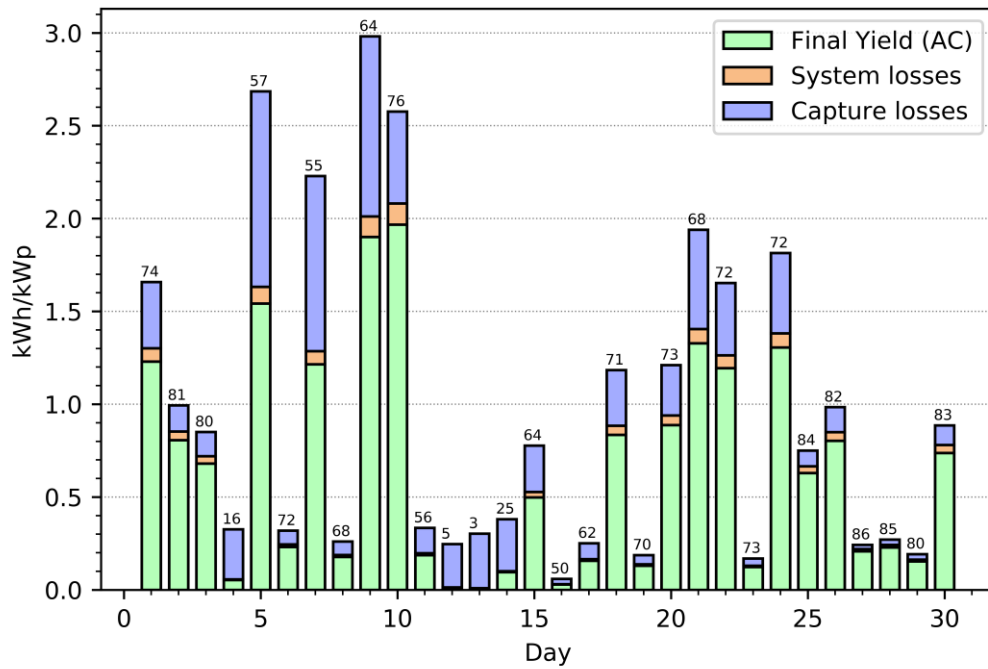
Month 9: energy output 4677 kWh

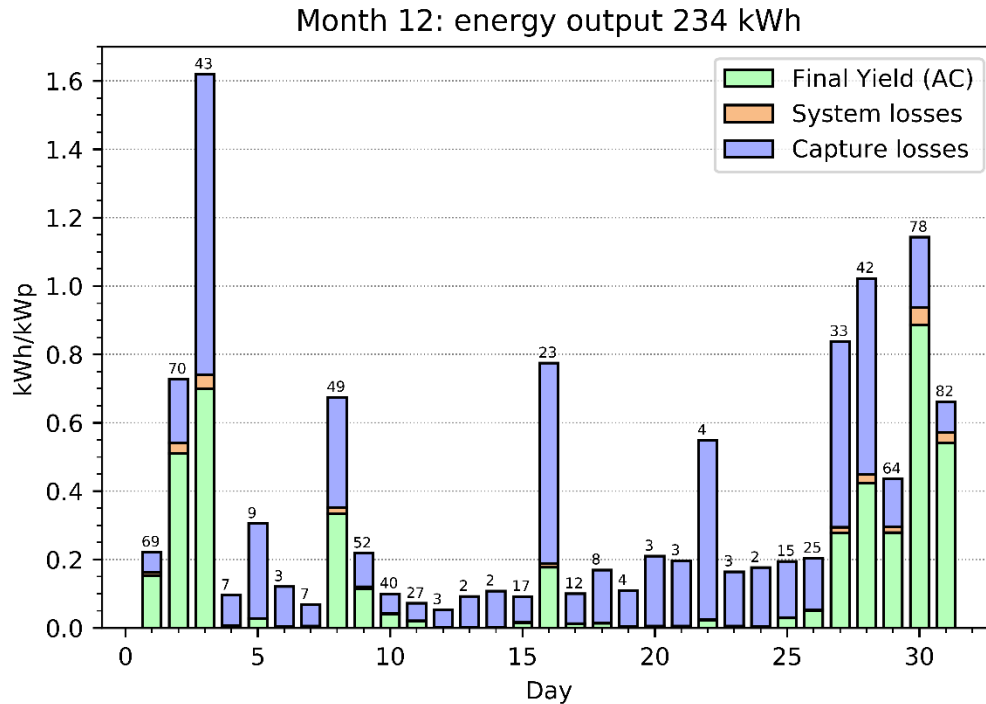


Month 10: energy output 2865 kWh



Month 11: energy output 972 kWh





## 7 References

- [1] "Penetrator Screw Anchors," American Earth Anchors, [Online]. Available: <https://americaneearthanchors.com/products/ground-anchors-penetrators/>. [Accessed 10 February 2020].
- [2] "University of Oregon Solar Radiation Monitoring Laboratory," [Online]. Available: <http://solardat.uoregon.edu/index.html>. [Accessed 2 March 2020].
- [3] "Aeronet Aerosol Robotic Network," NASA Goddard Spaceflight Centre, [Online]. Available: [https://aeronet.gsfc.nasa.gov/new\\_web/index.html](https://aeronet.gsfc.nasa.gov/new_web/index.html). [Accessed 2 March 2020].
- [4] "Atmospheric Soundings," University of Wyoming, College of Engineering, Department of Atmospheric Science, [Online]. Available: <http://weather.uwyo.edu/upperair/sounding.html>. [Accessed 2 March 2020].
- [5] F. Vignola, J. Michalsky and T. Stoffel, Solar and Infrared Radiation Measurements, Boca Raton: CRC Press, 2017.
- [6] Government of Canada, "Provincial and Territorial Energy Profiles - Yukon," Canada Energy Regulator, [Online]. Available: <https://www.cer-rec.gc.ca/nrg/ntgrtd/mrkt/nrgsstmprfls/yt-eng.html>. [Accessed 7 September 2020].
- [7] T. Huld, G. Friesen, A. Skoczek, R. P. Kenny, T. Sample, M. Field and E. D. Dunlop, "A power-rating model for crystalline silicon PV modules," *Solar Energy Materials and Solar Cells*, pp. 3359 - 3369, 2011.